Unraveling the Active Conformation of Urotensin II

Alfonso Carotenuto,[#,†] Paolo Grieco,[§] Pietro Campiglia,[§] Ettore Novellino,[§] and Paolo Rovero*[,#,‡]

Department of Pharmaceutical Sciences, University of Salerno, Via Ponte Don Melillo 11C, I-84084 Fisciano, Italy, and Department of Pharmaceutical and Toxicological Chemistry, University of Naples "Federico II", I-80131 Naples, Italy

Received August 6, 2003

Urotensin II (U-II) is a disulfide-bridged undecapeptide recently identified as the ligand of an orphan G-protein-coupled receptor. Human U-II (H-Glu-Thr-Pro-Asp-cyclo[Cys-Phe-Trp-Lys-Tyr-Cys]-Val-OH) has been described as the most potent vasoconstrictor compound identified to date.With the aim of elucidating the active conformation of hU-II, we have performed a spectroscopic analysis of hU-II minimal active fragment hU-II(4−11) in different environmental conditions. The analysis indicated that hU-II(4−11) was highly structured in the anisotropic membrane mimetic SDS solution, showing a type II′ β-turn structure, which is almost unprecedented for L-amino acid peptides. Micelle bound structure of hU-II(4−11) was then compared with those of four synthetic analogues recently synthesized in our lab, bearing modified Cys residues at position 5 and/or position 10 and characterized by different levels of agonist activity. The structures of the active compounds were found to be very similar to that of hU-II(4−11), while a barely active compound does not show any propensity to β-turn formation. Furthermore, distances among putative pharmacophoric points in the structures of the active compounds obtained in SDS solution are in good agreement with those found in a recently described non-peptide agonist of the hU-II receptor. A type II′ β-turn structure was already found for the somatostatin analogue octreotide. On the basis of the similarity of the primary and 3D structures of U-II and somatostatin analogues and on the basis of the sequence homology between the GPR14/UT-II receptor and members of the somatostatin receptor family, a common evolutionary pathway for the signal transmission system activated by these peptide can be hypothesized.

Introduction

Urotensin II (U-II) is a cyclic peptide originally isolated from the urophysis, the hormone storage−secretion organ of the caudal neurosecretory system of teleost fishes, and sequenced more than 20 years ago.[1] Several analogues of U-II have subsequently been reported in different species of fish and amphibians, with variations occurring in the five to seven N-terminal residues, followed by a C-terminal-conserved disulfide-bridged cyclic hexapeptide. Recently, urotensin II was cloned in several mammalian species, including humans.[2] Human U-II (hU-II) is an 11 amino acid peptide that retains the cyclic portion typical of fish U-II.

In 1999 Ames et al.[3] identified a new human G-protein-coupled receptor homologous to the GPR14/SENR orphan receptor from rat.[4] The use of a "reverse molecular pharmacology" approach[5] identified U-II as the ligand of this orphan receptor, now termed UT-II receptor.[6a] Interestingly, three other independent groups reported similar results within 2 months.[6b−d] As a result, there has been continued interest in U-II sequences, and various studies aiming at investigating the (patho)physiological role played by this peptide in mammals have shown that hU-II produces a very potent vasoconstriction of cynomolgus monkey arteries and human arteries and veins and potently contracts certain blood vessels from other species, such as the rat thoracic aorta.[3,7−9] hU-II has been shown to be 1−2 orders of magnitude more potent than endothelin-1 in producing vasoconstriction in mammals and thus is one of the most effective vasoconstrictor compounds identified to date.[3,10] Moreover, hU-II produces contractions in a number of nonvascular smooth muscle tissues, such as primate airways[11] and human heart.[12] On the basis of its spectrum of activities, hU-II has been postulated to contribute as modulator to cardiovascular homeostasis and possibly to be involved in certain cardiovascular pathologies.[9,13] In terms of drug development, it thus appears that a hU-II antagonist could be of therapeutic value in a number of cardiovascular disorders characterized by increased vasoconstriction, myocardial dysfunction, and even atherosclerosis. Unfortunately, as the biological studies on hU-II progress, limited structure−activity relationship is available to provide information on the residues responsible for the activity of this sequence.[14] Accordingly, in this study we have investigated the conformational properties of hU-II and its minimal active fragment hU-II(4−11) in different environmental conditions, comparing the obtained structures with those of active analogues bearing modified Cys residues at position 5 and/or position 10. In particular, the following peptides were considered (Table 1): (a) the recently described **P5U** superagonist, where Cys residue in position 5 was replaced by Pen (this peptide showed higher affinity than hU-II at human cloned U-II receptors as well as higher activity in the rat thoracic aorta assay[15]); (b) the analogue in which both Cys[5] and Cys[10] were substituted by Pen residues

* To whom correspondence should be addressed. Phone: +39 089 962809. Fax: +39 089 962828. E-mail: rovero@unisa.it.

[#] University of Salerno.

[†] Present address: Università di Napoli "Frederico II", Dip. Chimica Farmaceutica e Toss., Via D. Montesano 49, 80131, Naples, Italy. E-mail: alfonso.carotenuto@unina.it.

[§] University of Naples "Federico II".

[‡] Present address: Università di Firenze, Polo Scientifico, Via dell Lastruccia 13, I-50019 Sesto Fiorentino, Firenze, Italy. E-mail: paolo.rovero@unifi.it.

10.1021/jm0309912 CCC: $27.50 © 2004 American Chemical Society
Published on Web 02/19/2004

Table 1. Receptor Affinity and Biological Activity of Urotensin-II Analogues of General Formula R-Asp-c[Xaa-Phe-Trp-Lys-Tyr-Yaa]-Val-OH[a]

peptide	Xaa	Yaa	pK_i [b]	pD_2 [c]
hU-II	Cys	Cys	9.1 ± 0.08	8.3 ± 0.06
hU-II(4−11)	Cys	Cys	9.6± 0.07	8.6 ± 0.04
P5U	Pen	Cys	9.7± 0.07	9.6 ± 0.07
1	Pen	Pen	8.9 ± 0.11	8.2 ± 0.12
2	Cys	Pen	7.9 ± 0.04	6.7 ± 0.06
3	Cys	Hcy	nt[d]	<6.5

[a] R = H-Glu-Thr-Pro for hU−II; R = H for hU-II analogues. [b] p*Ki*: $-\log K_i$. [c] pD_2: $-\log EC_{50}$. Each value in the table is the mean ± sem of at least four determinations. [d] Not tested.

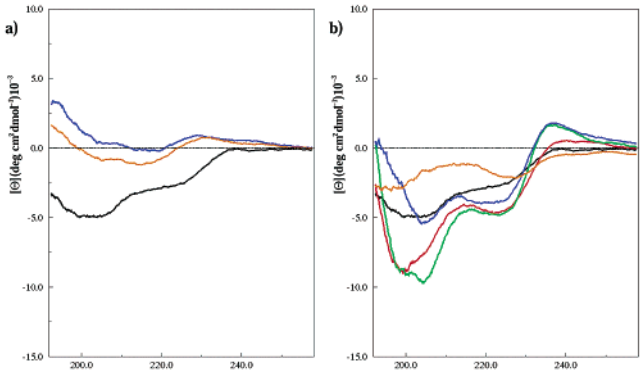

Figure 1. CD spectra of investigated peptides: (a) hU-II(4−11) in water (blue), water/HFA 1:1 v:v (orange), and SDS micelles solution (black); (b) CD spectra in SDS micelles solution of hU-II(4−11) (black), **P5U** (red), **1** (green), **2** (blue), and **3** (orange).

(compound **1**), which is almost as active as hU-II; (c) analogue **2** (Cys[10] replaced by Pen), whose activity dropped by 2 orders of magnitude; (d) the analogue in which Cys[10] was substituted by hCys (compound **3**), which resulted in very low activity.[16]

Results

CD Spectroscopy. To explore the conformational behavior of hU-II and its analogues, we first performed a CD study of the hU-II minimal active fragment hU-II(4−11) in various solution environments. The CD spectra of hU-II(4−11) were recorded in water, in HFA/water 50/50 v:v, and in SDS/water solutions (Figure 1a). CD spectra of hU-II(4−11) in water and HFA/water suggest the presence of disordered conformers with comparable amounts of random coil, turn, and β structures. These results are in line with previous NMR studies on teleostean fish U-II in DMSO solution,[17] on hU-II in water,[18] and in DMSO solution[19] that indicated the absence of defined secondary structures in the cyclic conserved portion of hU-II. In contrast, in aqueous SDS micelle solution (200 mM) the shape of the CD spectrum of hU-II(4−11) suggests the presence of β-turns and/or β-strands folding with a minimum at 205 nm and a shoulder around 215 nm. Peptides **P5U**, **1**, and **2** show similar CD spectra in SDS micelles, while the CD spectrum of peptide **3** under the same conditions is very different, indicating that this peptide is devoid of the ordered structure typical of hU-II(4−11) (Figure 1b).

NMR Analysis in SDS Micelles. The CD investigation described above was followed by the collection of a whole set of 1D and 2D NMR spectra in 200 mM aqueous solution of SDS for hU-II(4−11), hU-II, **P5U**, and peptides **1**−**3**. To check for the absence of an aggregation state of the peptides, spectra were acquired in the concentration range of 0.2−5 mM. No significant changes were observed in the distribution and in the shape of the ^{1}H NMR resonances, indicating that no aggregation phenomena occurred in this concentration range. Complete ^{1}H NMR chemical shift assignments were effectively achieved for all the analyzed peptides (Supporting Information) according to the Wüthrich procedure[20] via the usual systematic application of DQF-COSY,[21] TOCSY,[22] and NOESY[23] experiments with the support of the XEASY software package.[24] ^{13}C NMR Cα chemical shifts were determined by analysis of proton detected ^{1}H−^{13}C HSQC[25] (Supporting Information).

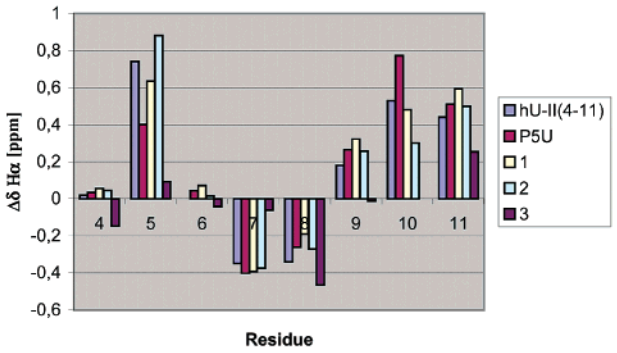

Figure 2. Secondary shifts of the α protons of the studied peptides in aqueous solution (pH 5.5) in the presence of SDS (200 mM) micelles. Pen Hα random coil value (4.65 ppm) was taken from ref 27c.

hU-II(4−11) in SDS Micelles. A qualitative analysis of short- and medium-range NOEs, $^3J_{NH-H\alpha}$ coupling constants, NH exchange rates, and temperature coefficients for exchanging NH was used to characterize the secondary structure of hU-II(4−11) (Supporting Information). The presence of a β-turn encompassing residues 6−9 is suggested by a weak H_α−NH_{i+2} connectivity between Trp[7] and Tyr[9] and a strong NH−NH_{i+1} connectivity between Lys[8] and Tyr[9]. Relatively strong $H_{\beta s}$−NH_{i+2} connectivities between Trp[7] and Tyr[9] indicate that this is not a canonical type I or type II β-turn, which are usually observed for natural L-amino acids. A turn structure is supported by the observation of slowly exchanging NH at position 9, a low value of the temperature coefficient for this proton ($-\Delta\delta/\Delta T$ < 3.0 ppb/K), and a small $^3J_{NH-H\alpha}$ coupling constant (<5 Hz) for residue Trp[7]. A short stretch of antiparallel β-sheet involving residues 5−6 and 10−11 is inferred from a number of long-range NOEs including H_α−NH connectivities between residues 5, 11 and 6, 10 and a NH−NH connectivity between residues 6 and 9. The structure formed by a β-turn flanked by an antiparallel β-sheet is henceforth referred to as a β-hairpin. The presence of a β-hairpin is supported by the observation of large $^3J_{NH-H\alpha}$ coupling constants (≥8 Hz) for Cys[5], Tyr[9], and Cys[10] and slowly exchanging NH at position 6. Additional evidence for β-hairpin formation is provided by the analysis of the H_α and C_α resonances, which are strongly dependent on local secondary structure.[26] Upfield shifts for H_α relative to random coil values are generally found for residues implicated in a α-helix or in turns and downfield shifts for those in β-sheets; the contrary is found for C_α shifts. As shown in Figure 2, H_α-7 and H_α-8 experience upfield shifts of the NMR

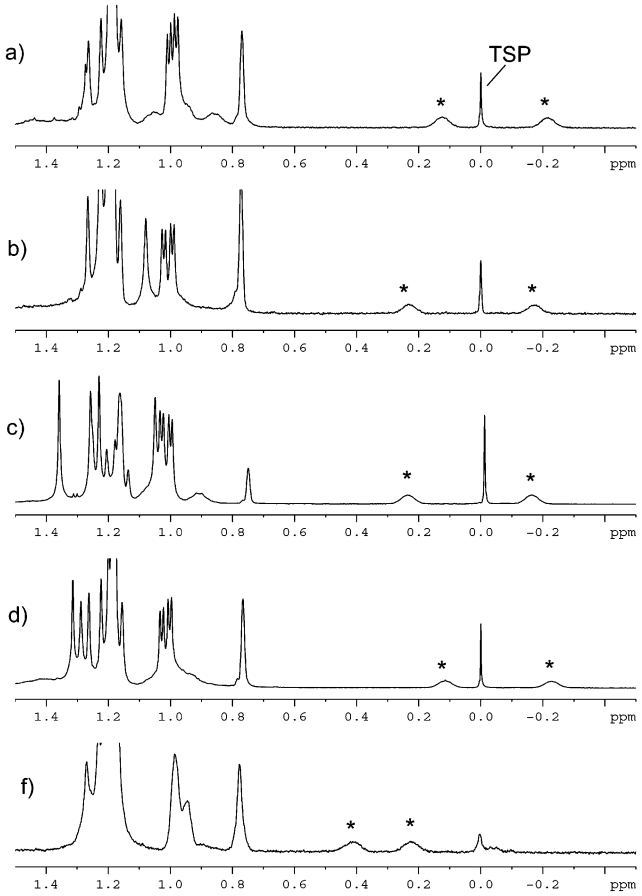

Figure 3. Upfield region of the 1D ^{1}H NMR spectra of compounds (from top to bottom): hU-II(4−11) (a), **P5U** (b), **1** (c), **2** (d), **3** (e). Hγ resonances of Lys^8 are indicated with a star.

signals compared to those observed for the same amino acids in random coil state, while Cys^5, Tyr^9, and Cys^{10} H$_\alpha$ experience downfield shifts; accordingly, Trp^7 C$_\alpha$ experiences a downfield shift, while Phe^6, Tyr^9, and Cys^{10} C$_\alpha$ resonances are upfield-shifted (Supporting Information). Consistent with the CD results, all these data indicate the presence of a β-hairpin in the region encompassing residues 5−10 with a turn at positions Trp^7-Lys^8. Finally, a dramatic upfield shift is observed for H$_\gamma$ atoms of Lys^8, (δ −0.16 and δ 0.18 ppm, with a $\Delta\delta$ of about −1.5 ppm relative to Lys H$_\gamma$ resonances in random coil peptides). Such an impressive shielding (Figure 3) is probably due to the influence of Trp^7 and Tyr^9 aromatic ring currents on the Lys^8 H$_\gamma$ atoms. Actually, several interchain connectivities observed in the NOESY spectrum indicate that the Lys^8 side chain is spatially close to Trp^7 and Tyr^9 aromatic side chains.

hU-II in SDS Micelles. The ^{1}H NMR spectra of hU-II in SDS micelles show a doubling of all the resonances, indicating equilibrium between two different states that exchange slowly on the NMR time scale. The relative intensities of resolved amide proton signals indicate a ratio of 3:1 between the two states. The resonances of the protons of both states could be assigned using the usual procedure[20] (Supporting Information). Luckily, the conformational equilibrium produces resolved peaks for almost all resonances. One of the two states, the most populated one, shows spectral features resembling those found for hU-II(4−11), with similar NH exchange rates, NH temperature coefficients, $^3J_{NH-H\alpha}$ coupling constants, NOE connectivities, and proton resonances, with the exception of those of Asp^4 and Cys^5 residues, which obviously feel the effect of N-terminal residues. In contrast, the less populated state shows a minor number of NOE contacts per residue, without medium- and long-range diagnostic NOEs, and it also shows fast exchanging rates for all the amide protons. These data indicate that the second set of signals arises from a more flexible structure. Additional support for random structure is provided by the analysis of the H$_\alpha$ chemical shifts, which closely resemble those of random coil peptides (data not shown). The resonance values of the protons belonging to this second conformer also significantly differ from the corresponding in water solution (Supporting Information). Furthermore, changing of the peptide and/or the micelle concentrations did not change the ratio between the populations of the two states of the peptide. Thus, it is possible that hU-II binds to the micelles in two different conformations, the first being highly structured and the second more flexible. The minor conformer was not considered in the following structure calculation procedures.

P5U in SDS Micelles. P5U shows spectral features resembling those found for hU-II(4−11), with similar NH exchange rates, NH temperature coefficients, $^3J_{NH-H\alpha}$ coupling constants, NOE connectivities, and proton and carbon resonances for unchanged residues. The differences between the NMR data of **P5U** and hU-II(4−11) point to a higher conformational stability in the first. In particular, we observed a higher number of medium-range NOE connectivities (24 NOE/residue for **P5U** against 15 NOE/residue for hU-II(4−11)) and longer NH exchange times for residue 6, indicating that this NH is engaged in a stronger hydrogen bond, stabilizing the hairpin structure. Additional support for this stronger hydrogen bond arises from the downfield shift of the resonance of the residue 6 amide proton in **P5U** compared to the relevant resonance in hU-II(4−11) (9.18 and 9.01 ppm, respectively).

Peptide 1 in SDS Micelles. Peptide **1** shows spectral features resembling those found for hU-II(4−11) and **P5U**, indicating the presence of the hairpin structure. Detailed investigation on NH exchange rates, NH temperature coefficients, $^3J_{NH-H\alpha}$ coupling constants, and NOE connectivities (Supporting Information) indicates that the hairpin structure in **1** is further strengthened compared to hU-II(4−11) and **P5U**. In fact, after dissolution of lyophilized samples in ^2H_2O micelle solution, the residue 9 NH signal totally disappears in 2 days for hU-II(4−11) and **P5U** while the corresponding proton signal in **1** is still observable after 1 month. A further relevant difference between **1** and hU-II(4−11) (or **P5U**) is the observation in the first of a long exchange time for the NH of residue 11. This finding, together with a number of NOE connectivities between Asp^4 and Val^{11}, indicate that the N- and C-terminal residues of **1** are part of the hairpin structure.

Peptide 2 in SDS Micelles. Peptide **2** shows spectral features resembling those found for the above-described peptides. Slow exchange rates observed for NH of residues 6, 8, 9, and 11 indicate a structure more similar to the structure of peptide **1**, with a β-hairpin motif

extending from Asp[4] to Val[11] although the overall data indicate a higher degree of flexibility in **2** relative to **1**. A remarkable difference from comparing NMR data of **2** with those of all the above-described peptides is represented by the exchange rate of Lys[8] NH, which is slow in **2** while it is relatively fast in the other peptides. Furthermore, in **2** the resonances of the Lys[8] Hγ's are even more shielded compared to the corresponding ones in hU-II(4−11), **P5U**, and **1** (Figure 3). These spectral features indicate that some differences are possible in the structure of the turn region.

Peptide 3 in SDS Micelles. All the spectral features of peptide **3** indicate a high degree of flexibility for this peptide. $^3J_{NH-H\alpha}$ coupling constants falling between 5 and 8 Hz, the small number of NOE contacts per residue, the absence of medium- and long-range diagnostic NOE's, together with H_α chemical shift values close to random coil peptides (Figure 2), clearly indicate a disordered conformation.

Structure Calculations. NMR-derived constraints for hU-II(4−11), hU-II, **P5U**, and peptides **1**−**3** were used as the input data for a simulated annealing structure calculation as implemented within the standard protocol of the DYANA program.[27] In the first step, only NOE-derived constraints were considered. NOEs were translated into interprotonic distances and used as upper limit constraints in subsequent annealing procedures to produce 200 conformations. From these structures we could unequivocally determine the hydrogen bond atom acceptors corresponding to the slowly exchanging NH previously determined for each peptide. In a second DYANA run these hydrogen bonds were explicitly added as upper and lower limit constraints, together with the NOE-derived constraints. The annealing procedure produced 200 conformations from which 50 structures were chosen, whose interprotonic distances best fitted NOE-derived distances, and then refined through successive steps of restrained and unrestrained EM calculations using the program Discover (Biosym, San Diego, CA). For each peptide, 20 structures satisfying the NMR-derived constraints (violations smaller than 0.27 Å) were chosen for further analysis (Figures 4 and 5). The PROMOTIF program was used to extract details of the location and types of structural secondary motifs.[28] The rms deviation values of the 20 calculated structure family for each peptide are reported in the Supporting Information (Table 1).

Solution Structure of hU-II(4−11) in SDS Micelles. As expected from the high number of NMR constraints, the hexacyclic region of hU-II(4−11) was well defined, possessing an average rms deviation of the backbone heavy atoms equal to 0.22 Å (Figure 4a). Side chain orientations of the residues belonging to this region were also defined (the average rms deviation for all non-hydrogen atoms was 0.46 Å). The two residues located outside the cycle were less defined (overall heavy atoms rms deviation of 0.90 Å), indicating higher conformational freedom for these residues. The analysis of the secondary structure showed the existence of a β-hairpin structure encompassing residues 5−10 with a βII′-turn conformation about residues Phe[6]-Trp[7]-Lys[8]-Tyr[9]. This well-conserved region is stabilized by hydrogen bonds between Phe[6] NH and Tyr[9] CO and between Phe[6] CO and Tyr[9] NH. The determined inverse turn

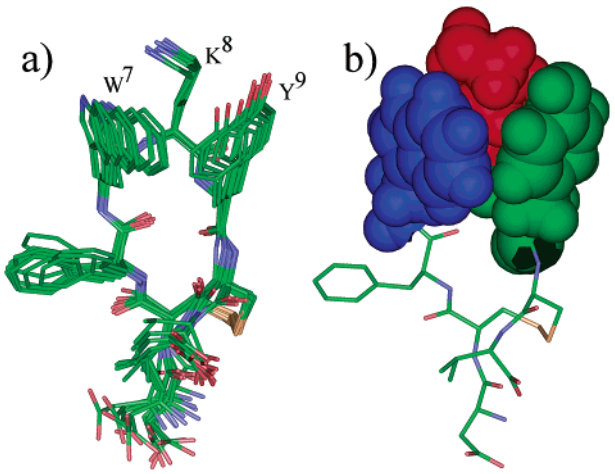

Figure 4. (a) Superposition of the 10 lowest energy conformers of hU-II(4−11). Structures were superimposed using the backbone heavy atoms of residues 5−10. Heavy atoms are shown with different colors (carbon, green; nitrogen, blue; oxygen, red; sulfur, gold). Hydrogen atoms are not shown for clarity. (b) Representative structure of hU-II(4−11) (i.e., the structure most similar to the mean of the 10 final structures). The Trp[7] (blue), Lys[8] (red), and Tyr[9] (green) side chains are shown as van der Waals surfaces.

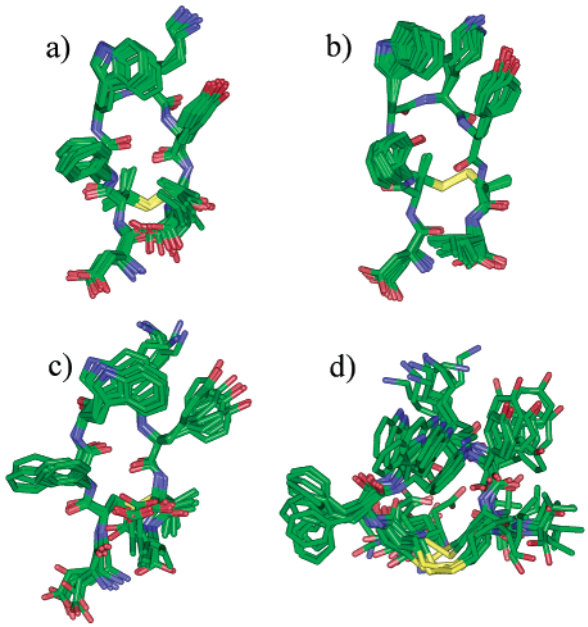

Figure 5. Superposition of the 10 lowest energy conformers of **P5U** (a), **1** (b), **2** (c), **3** (d). Structures were superimposed using the backbone heavy atoms of residues 5−10. Heavy atoms are shown with different colors (carbon, green; nitrogen, blue; oxygen, red; sulfur, gold). Hydrogen atoms are not shown for clarity.

conformation is unexpected for an all-L peptide. In fact, among natural amino acids, only glycine has been found at position $i + 1$ of a βII′-turn conformation, although Weiβhoff et al.[29] have recently reported an all-L cyclic pentapeptide showing a βII′-turn conformation in DMSO solution with a threonine residue at position $i + 1$. Analysis of the Ramachandran plot of the calculated conformations shows that all the residues lie in allowed regions except the Trp[7] residue, which lies in a generously allowed region. The structures do not show any van der Waals repulsion. To assess the overall stability of the obtained micelle bound structure of hU-II(4−11),

Table 2. Pharmacophoric Distances[a] (Å) of UT-II Receptor Agonists

peptide	$Trp^{7\,b}$-$Lys^{8}N\epsilon(Q\gamma)$	$Trp^{7\,b}$—$Tyr^{9\,b}$	$Lys^{8}N\epsilon(Q\gamma)$—$Tyr^{9\,b}$
hU-II(4−11)	5.4 (3.6)	5.8	6.0 (3.7)
P5U	5.6 (3.50)	6.1	6.2 (3.9)
1	5.8 (3.5)	6.3	6.1 (3.9)
2	4.8 (3.0)	5.8	6.6 (4.1)
AC-7954 (**A**)	5.5	6.6	6.2
AC-7954 (**B**)	7.2	5.2	6.1
U-II[c]	11.3	12.2	6.4
DTrp U-II[c]	13.7	8.3	11.1

[a] Reported distances were the mean of the 20 calculated structures of each peptide. [b] Aryl ring centroids. [c] See ref 19.

we subsequently performed a totally unrestrained molecular dynamic simulation. The results of this simulation indicate a high stability of the βII′-turn conformation (see below). In Figure 4b the side chains of Trp^{7}, Lys^{8}, and Tyr^{9} residues are evidenced as van der Waals surfaces. Clearly, the side chains of these residues are spatially close, and their mutual orientations justify the considerable upfield shift observed for Hγ atoms of Lys^{8} (Figure 3). The distance defining the putative hU-II pharmacophore according to Fhlor's three-point pharmacophore hypothesis[18] is reported in Table 2.

Solution Structure of hU-II in SDS Micelles. As assessed above, two different conformational states could be observed for hU-II in SDS micelles by NMR experiments. The overall NMR data of the less populated state indicate a random structure; therefore, this state has not been considered for structure calculations. The most populated state, possessing spectral features resembling those found for hU-II(4−11), when submitted to the structure calculation steps described above, gave a 3D structure of the cyclic region virtually undistinguishable from that of hU-II(4−11) (data not shown). Preliminary results on the micelle bound structure of hU-II have been recently presented.[30]

Solution Structure of P5U and Peptides 1−3 in SDS Micelles. Figure 5 shows the calculated structures of hU-II(4−11) analogues. The rms deviations of the cyclic and overall heavy atoms are reported in the Supporting Information (Table 1). **P5U** and peptides **1** and **2** show a 3D structure similar to that of hU-II(4−11) with a β-hairpin structure encompassing residues 5−10 and a βII′-turn conformation about residues Phe^{6}-Trp^{7}-Lys^{8}-Tyr^{9}. Some interesting points can be outlined: (i) A significant enhancement of the conformational rigidity is observed in the calculated structures of **P5U** (Figure 5a) compared to hU-II(4−11), in accordance with experimental data. (ii) An overall enhancement of the conformational rigidity is observed for peptide **1** compared to hU-II (4−11) and **P5U** (Figure 5b). Furthermore, this analogue possesses a β-hairpin structure encompassing all residues, included N- and C-terminal ones. (iii) A thorough investigation of the peptide **2** structure (Figures 5c and 6) reveals that the Trp^{7} indole moiety is spatially closer to the Lys^{8} side chain, while the Tyr^{9} phenol ring is slightly more distant from the same alkylamine side chain compared to the corresponding distances in hU-II(4−11) and **P5U** (Table 2). (iv) A high degree of flexibility was observed for peptide **3** (Figure 5d). No standard pattern of secondary structures was observed in any calculated structure of **3**, and these results clearly evidenced disordered conformations.

Molecular Dynamics Simulations of hU-II(4−11), P5U, and Peptides 1 and 2. According to the conformational analysis described above, the membrane mimetic environment forces peptides hU-II(4−11), **P5U**, **1**, and **2** to fold in a βII′-hairpin structure, which is quite unexpected for an all-L peptide. To assess the absolute structural stability of this inverse turn, regardless of the environmental constraints, the dynamic behavior of all the active analogues was investigated in detail by molecular dynamics simulations *in a vacuum*. To this end, we performed four 300 ps of unrestrained MD simulations starting from the lowest energy NMR structure of each peptide. The stability of the βII′-turn structure was followed by monitoring the ϕ and ψ dihedral angle values of residues Trp^{7} and Lys^{8}. The ϕ and ψ dihedral angles defining the type II′ β-turn are quite stable during the entire simulation time (Supporting Information), indicating that the βII′-turn represents a local minimum, regardless of the application of constraints. On the basis of the dynamical properties of the analyzed peptides, we conclude that peptide **1** shows the most rigid structure with an overall heavy atoms rms deviation of 0.72 Å (calculated considering 20 structures sampled every 15 ps of the MD simulation), while hU-II (4−11), **P5U**, and peptide **2** show rms deviations of 1.32, 0.94, and 1.44 Å, respectively.

Structural Comparison of hU-II with AC-7954, the First Non-Peptide U-II Receptor Agonist. The conformations accessible to biologically active ligands in solution are not necessarily the same as those adopted by the same ligands when bound to their receptors; henceforth, the biological relevance of NMR-derived 3D structures of peptides always has to be validated. A straightforward method to assess the biological relevance of NMR-derived 3D structures of peptides is their superposition with 3D structure(s) of non-peptide rigid ligand(s). The first and, to the best of our knowledge, the only non-peptide UT-II receptor agonist reported in the literature is the compound termed AC-7954 [(±)3-(4-chlorophenyl)-3-(2-(dimethylamino)ethyl)isochroman-1-one hydrochloride].[31] To explore the conformational behavior of this compound, it was submitted to extended MD calculations (see Experimental Section). Analysis of the MD data revealed that the compound exists in two interconverting pseudochairs with the ethylamine or the 4-chlorophenyl functions in pseudoaxial position, termed conformers **A** and **B**, respectively. Both conformers have similar energy (108.0 kcal/mol for **A**, and 106.4 kcal/mol for **B**, CVFF force field[32]). Considering as pharmacophoric points of AC-7954 the nitrogen atom, the centroid of the chlorophenyl aromatic ring, and the centroid of the isochromanone aromatic ring, we compared the distance among these (pseudo)atoms to the "corresponding" ones in the bioactive peptides, where the isochromanone was considered to correspond to the tryptophan indole ring due to the presence of the oxygen heteroatoms that could mimic the nitrogen of the indole. As shown in Table 2, the agreement among the distances in the pharmacophore is good for both the AC-7954 conformers. In particular, considering the lowest energy conformer **A**, the differences in the pharmacophoric distances are within 0.5 Å when compared with the most active peptide **P5U**. In Figure 7, a side by side view of a calculated structure

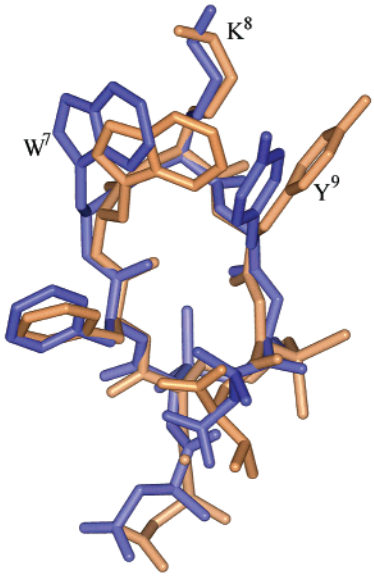

Figure 6. Superposition of the most representative structure of **P5U** (blue) with the corresponding one of peptide **2** (gold). Structures were superimposed using the backbone heavy atoms of residues 5−10. Hydrogen atoms are not shown for clarity.

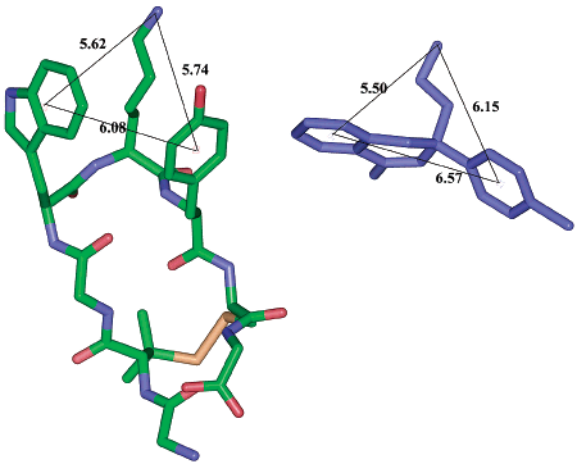

Figure 7. Side by side view of **P5U** (the most representative NMR structure) and of the (*R*)-AC-7954 conformer **A**. Putative pharmacophoric distances are indicated in angstroms. All hydrogen atoms and the side chains of residues 4, 6, and 11 of **P5U** are not shown for clarity.

of AC-7954 conformer **A** and a representative micelles bound structure of **P5U** is shown.

Discussion

The structural requirements of U-II for receptor activation were studied throughout an extensive spectroscopic analysis of hU-II, its minimal active fragment hU-II(4−11), the highly active peptide agonist **P5U**, and other peptide agonists **1**−**3**. Initially, the conformational behavior of hU-II(4−11) was explored under different environmental conditions by CD spectroscopy. In particular, CD studies on hU-II(4−11) were performed in water, in water/HFA 50/50 v:v, a mixture that can probe the intrinsic tendency of the peptide to assume helical conformation,[33] and in anisotropic SDS−micelles medium as a membrane mimetic environment. CD data clearly indicate that the highest degree of structural definition is shown in the membrane-like environment (Figure 1a). On these bases, an extensive CD, NMR, and MD investigation was performed on distinct UT-II receptor peptide agonists hU-II(4−11), hU-II, **P5U**, **1**, **2**, and **3** in the lipid environment.

A type II′ β-hairpin structure was a common feature found in the highly active peptides hU-II(4−11), hU-II, **P5U**, and **1** and in the low-active **2**, while the very low-active peptide **3** is devoid of any defined structure (Figures 4 and 5). This βII′ structure is almost unprecedented for L-amino acid peptides, since it has been reported only for a highly constrained pentacyclic peptide.[29] Unrestrained MD simulations allowed us to verify the structural stability of this uncommon structural motif. Interestingly, the substitution of the L-Trp residue of hU-II with the D isomer, which stabilizes a type II′ β-turn, is tolerated in a receptor binding assay.[18]

A cluster involving the side chains of Trp[7], Lys[8], and Tyr[9] was a second noteworthy feature in the calculated conformation of UT-II receptor active peptides (Figure 4b). A detailed structure−activity relationship recently reported by Flohr and co-workers[18] showed that this Trp-Lys-Tyr sequence is the most important for full agonist activity of hU-II. In the same work, a three-point pharmacophore hypothesis was proposed: a positive ionizable feature placed on the Nϵ atom of Lys[8] and two hydrophobic aromatic features positioned onto the aryl rings of Trp[7] and Tyr[9]. Using the NMR structure of hU-II and D-Trp[7] hU-II, Flohr et al.[18] deduced distances between the pharmacophoric points to be used in a screening of the Aventis compound repository. These distances are quite different from those we have found in the most active peptide agonists (Table 2). The different environments in which these distances were obtained can account for this discrepancy. In fact, Flohr et al.[18] deduced the pharmacophoric distances in isotropic aqueous medium, while our distances were deduced in a membrane mimetic environment. The use of SDS micelles to study the conformational properties of hU-II and hU-II analogues is motivated on the basis of their interaction with a membrane receptor. For peptides acting as ligand of membrane receptors, the use of membrane mimetic media, such as SDS or dodecylphosphocoline, is suggested hypothesizing a membrane-assisted mechanism of interactions between the peptides and their receptors.[34] According to this model, the membrane surface plays a key role in facilitating the transition of the peptide from a random coil conformation adopted in the extracellular environment to a conformation that is recognized by the receptor.[35] The increase of the local concentration and the reduction of the rotational and translational freedom of the neuropeptide are membrane-mediated events acting as determinant steps for the conformational transition of the peptide.[36] Our pharmacophoric model was then validated by comparing the obtained pharmacophoric distances with the corresponding ones in the compound AC-7954, the first and, to the best of our knowledge, the only non-peptide U-II receptor agonist reported in the literature.[31] As shown in Figure 7, the differences in the pharmacophoric distances in AC-7954 are within 0.5 Å, compared to those of the most active peptide **P5U**. Although Flohr et al.[18] screened the Aventis database using pharmacophoric distances from compounds with agonist activity, the search led to compounds with

antagonist activity, while it is well-known that antagonist topographical requirements are usually very different from those defining the agonist activity.

The NMR-derived 3D structures of compounds hU-II(4−11), **P5U**, and **1**−**3** could explain their relative biological activities and receptor affinities (Table 1). In particular, the enhanced pharmacological properties observed in the case of **P5U** can be ascribed to the conformational restriction obtained by replacement of Cys by Pen in position 5, a modification that apparently favors the selection of a UT-II receptor bioactive conformation.[37] Peptide **1** shows receptor affinity and biological activity comparable to those of hU-II and slightly reduced compared to those of hU-II(4−11). The reduced pharmacological properties observed for **1** can be tentatively ascribed either to the exceptionally high conformational rigidity of this compound, which would prevent the peptide from reaching biologically significant conformations (i.e., postbinding structure transitions) or, more trivially, to steric hindrance of the Pen[10] methyl groups of **1** within the UT-II receptor binding site. The different distances between the side chains of the Trp-Lys-Tyr triad observed in **2** compared to the corresponding ones in hU-II(4−11) and **P5U** (Table 2 and Figure 6) can explain the reduced activity of **2** compared to the parent peptide hU-II(4−11), even if a steric hindrance of the Pen[10] methyl groups within the UT-II receptor binding site cannot be excluded, as in the case of peptide **1**. The loss of any propensity to the formation of definite structures in peptide **3** and, in particular, to the formation of the β-hairpin structure observed in the other active compounds could explain the very low activity of this peptide. Of note is that the presence in **3** of a single additional methylene group extending the disulfide bridge drastically reduces the conformational stability of the βII′ hairpin structure. Accordingly, we have recently reported[19] that the length of the bridge moiety in hU-II analogues is a key feature for the activity at the UT-II receptor.

A type II′ β-hairpin structure has been already found for the somatostatin analogue octreotide (sandostatin).[38] In octreotide, the D-configuration of the tryptophan residue at position $i + 1$ of the turn favors the inverse turn, and actually, this structural feature was observed in DMSO solution, although in equilibrium with helical structures. Figure 8 shows the superposition of the micelle bound structure of the superagonist **P5U** with that of octreotide (PDB entry 1SOC). The almost perfect overlapping of the backbone heavy atoms of the hairpin can be observed. Furthermore, the distance between the nitrogen atom of the side chain of the lysine residue and the centroid of the D-tryptophan indole moiety is 6.12 Å, closely resembling the corresponding distance in **P5U**. Interestingly, an upfield shift of the Lys[8] Hγ resonances has also been observed in the case of octreotide. The intensity of that shift in octreotide was smaller compared to that shown by **P5U**. This is probably due to one or more of the following octreotide features: (a) the absence of the Tyr[9] aromatic ring; (b) the greater distance between the Lys[8] Hγ and the centroid of the tryptophan indole moiety; (c) the observed equilibrium between β-hairpin and helical structures.[38] This 3D structural resemblance of the ligands, together with the similarity of the primary structure of

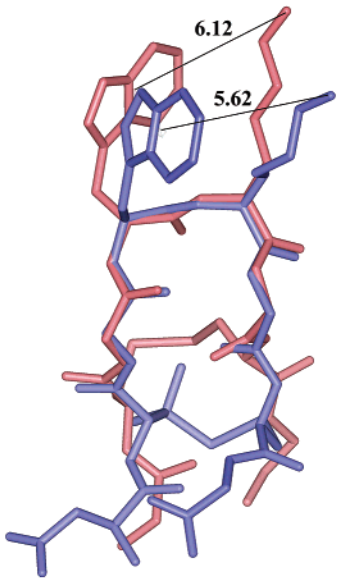

Figure 8. Superposition of the most representative structure of **P5U** (blue) with the octreotide structure (PDB entry 1SOC, pink). Structures were superimposed using the backbone heavy atoms of residues 5−10. Hydrogen atoms and the side chains of residue 4, 6, 9, and 11 are not shown for clarity.

U-II and somatostatin analogues, and the sequence homology between the GPR14/UT-II receptor and members of the somatostatin receptor family[6c] indicate similar structural requirements for the activation of these receptors, which in turn could have some implications in the evolutionary pathways for the signal transmission system activated by these peptides. Finally, it is worth mentioning that several octapeptide somatostatin antagonists have been recently found to function as a weak UT-II receptor antagonist,[39] again indicating structural similarities between UT-II and somatostatin receptors ligands.

Conclusions

In conclusion, a type II′ β-hairpin structure was a common feature found in the active peptides acting on the UT-II receptor. This structural arrangement allows a tight contact among the side chains of the indispensable residues; in order to obtain full agonist activity, the distances between the putative pharmacophoric points, the aryl ring of Trp[7] (A), the Nϵ of Lys[8] (B), and the aryl ring of Tyr[9] (C), must be the following: 5.4−5.8 Å (A−B), 5.8−6.2 Å (A−C), and 6.0−6.2 Å (B−C). This investigation offers a structural basis for the design of novel non-peptide agonists and, possibly, antagonists to be used as pharmacological probes in revealing the (patho)physiological role of U-II.

Experimental Section

Sample Preparation. Tested peptides were synthesized and purified as previously reported.[15,16] HFA and 99.9% ^2H_2O were obtained from Aldrich (Milwaukee, WI), 98% SDS-d_{25} was obtained from Cambridge Isotope Laboratories, Inc. (Andover, MA), and [(2,2,3,3-tetradeuterio-3-(trimethylsilanyl)]-propionic acid (TSP) was obtained from MSD Isotopes (Montreal, Canada).

Circular Dichroism. All CD spectra were recorded using a JASCO J810 spectropolarimeter with a cell path length of 1 mm. The CD measures were performed using a measurement range from 260 to 190 nm, 1 nm bandwidth, 8 accumulations,

and 10 nm/min of scanning speed at room temperature. The pH of the aqueous sample was adjusted to 5.5 by adding a small amount of phosphate buffer solution. Peptide concentration was determined spectrophotometrically using tyrosine and tryptophan absorbance as described.[40] For the hU-II(4−11) conformational exploration, 300 μL of a 1.0 mM water stock solution was prepared and the final 0.1 mM solutions were obtained adding 30 μL of the stock solution to the appropriate amount of buffered water, water and HFA, and 200 mM SDS aqueous solution. The SDS samples of the other tested peptides were obtained by dissolving the appropriate amount of these in a 200 mM SDS aqueous solution. Mean residue ellipticities were calculated for each sample by the usual method.[41]

NMR Spectrometry. The samples for NMR spectrometry were prepared by dissolving the appropriate amount of peptide in 0.45 mL of ^1H_2O (pH 5.5) and 0.05 mL of ^2H_2O to obtain 1−2 mM of peptides and 200 mM of SDS-d_{25}. HSQC experiments and the NH exchange studies were performed by dissolving peptides in 0.50 mL of ^2H_2O and 200 mM of SDS-d_{25}. TSP was used as the internal chemical shift standard. NMR spectra were recorded on a Bruker DRX-600 spectrometer. All spectra were recorded at a temperature of 300 K. One-dimensional (1D) NMR spectra were recorded in the Fourier mode with quadrature detection, and the water signal was suppressed by low-power selective irradiation in the homogated mode. 2D DQF-COSY,[22] TOCSY,[22] and NOESY[23] experiments were run in the phase-sensitive mode using quadrature detection in ω_1 by time-proportional phase increase of the initial pulse.[33] Data block sizes were 4096 addresses in t_2 and 512 equidistant t_1 values. Before Fourier transformation, the time domain data matrices were multiplied by shifted $\sin^2$ functions in both dimensions. A mixing time of 70 ms was used for the TOCSY experiments. NOESY experiments were run at 300 K with mixing times in the range of 150−300 ms. The spectra were calibrated relative to TSP (0.00 ppm) as the internal standard. The qualitative and quantitative analyses of DQF-COSY, TOCSY, and NOESY spectra were obtained using the interactive program package XEASY.[24] $^3J_{HN-H\alpha}$ values were obtained from 1D ^{1}H NMR and 2D DQF-COSY spectra. The temperature coefficients of the amide proton chemical shifts were calculated from 1D ^{1}H NMR and 2D DQF-COSY experiments performed at different temperatures in the range 300−320 K by means of linear regression.

Structural Determinations and Computational Modeling. The NOE-based distance restraints were obtained from NOESY spectra collected with a mixing time of 200 ms. The NOE cross-peaks were integrated with the XEASY program and were converted into upper distance bounds using the CALIBA program incorporated into the program package DYANA.[27] Cross-peaks that were overlapped by more than 50% were treated as weak restraints in the DYANA calculation. In the first step, only NOE-derived constraints (Supporting Information) were considered in the annealing procedures. For each examined peptide, 200 structures were generated with the simulated annealing standard protocol of the program DYANA.[27] Nonstandard Pen residues were added to DYANA residue library using MOLMOL.[42] From these structures, we could univocally determine the hydrogen bond atom acceptors corresponding to the slowly exchanging NH previously determined for each peptide. In a second DYANA run, these hydrogen bonds were explicitly added as upper and lower limit constraints (NH of Phe^6 with CO of Tyr^9, and NH of Tyr^9 with CO of Phe^6), together with the NOE-derived upper limit constraints (Supporting Information). The second annealing procedure produced 200 conformations from which 50 structures were chosen, whose interprotonic distances best fitted NOE-derived distances, and then refined through successive steps of restrained and unrestrained EM calculations. First, steepest descent minimizations with distance restraints were performed on all structures with the Discover algorithm (Biosym, San Diego, CA) utilizing the consistent valence force field (CVFF).[32] A generic distance maximum force constant of 100 kcal/mol and an upper distance force constant of 32 kcal/Å^2 were used. Minimization proceeded until the change in energy was less than 0.05 kcal/mol. This was followed by 3000 steps of unrestrained steepest descent energy minimization. A distance-dependent dielectric constant equal to 4r was applied to evaluate electrostatic interactions. The minimization lowered the total energy of the structures; no residue was found in the disallowed region of the Ramachandran plot. The final structures were analyzed using the InsightII program (Biosym, San Diego, CA). Graphical representation were carried out with the InsightII program (Biosym, San Diego, CA). The rms deviation analyses between energy-minimized structures were carried out with the program MOLMOL.[42] The PROMOTIF program was used to extract details on the location and types of structural secondary motifs.[28]

Molecular Dynamic Simulation. Peptides hU-II(4−11), **P5U**, **1**, and **2** were subjected to a molecular dynamic simulation using the Discover algorithm (Biosym, San Diego, CA) utilizing the consistent valence force field (CVFF).[32] The lower energy conformer obtained from the simulating annealing and following minimization procedures described above were subjected to 300 ps of molecular dynamics calculations after an equilibration period of 1 ps using a temperature of 300 K. During the molecular dynamics frame, structures were saved every 1 ps. A distance-dependent dielectric constant equal to 4r was applied to evaluate electrostatic interactions.

The AC-7954 structure of both enantiomers *R* and *S* was built with the builder module of InsightII (Biosym, San Diego, CA). The initial structure was first subjected to 3000 steps of steepest descent energy minimization and then to 300 ps of molecular dynamics calculations after an equilibration period of 1 ps using a temperature of 300 K. During the molecular dynamics frame, structures were saved every 1 ps. A distance-dependent dielectric constant equal to 4r was applied to evaluate electrostatic interactions.

Appendix

Abbreviations. Abbreviations used for amino acids and designation of peptides follow the rules of the IUPAC-IUB Commission of Biochemical Nomenclature in *J. Biol. Chem.* **1972**, *247*, 977−983. Amino acid symbols denote the L-configuration unless indicated otherwise. The following additional abbreviations are used: U-II, urotensin II peptide; SDS, sodium dodecyl sulfate; SAR, structure−activity relationship; NMR, nuclear magnetic resonance; CD, circular dichroism; HFA, hexafluoroacetone trihydrate; DMSO, dimethyl sulfoxide; DQF-COSY, double-quantum-filtered correlation spectroscopy; TOCSY, total correlation spectroscopy; NOESY, nuclear Overhauser enhancement spectroscopy; NOE, nuclear Overhauser effect; HSQC, heteronuclear single quantum correlation spectroscopy; MD, molecular dynamics; EM, energy minimization; 1D, one-dimensional; 2D, two-dimensional; 3D, three-dimensional; hCys, homocysteine; Pen, pennicillamine; TSP, 3-(trimethylsilanyl)propionic acid.

Supporting Information Available: NMR data of the analyzed peptides, rms deviations of the calculated structures, and details on the molecular dynamics simulations. This material is available free of charge via the Internet at http://pubs.acs.org.

References

(1) Pearson, D.; Shively, J. E.; Clark, B. R.; Geschwind, I. I.; Barkley, M.; Nishioka, R. S.; Bern, H. A. Urotensin II: a somatostain-like peptide in the caudal neurosecretory system of fishes. *Proc. Natl. Acad. Sci. U.S.A.* **1980**, *77*, 5021−5024.

(2) Coulouarn, Y.; Lihrmann, I.; Jegou, S.; Anouar, Y.; Tostivint, H.; Beauvillain, J. C.; Conlon, J. M.; Bern, H. A.; Vaudry, H. Cloning of the cDNA encoding the urotensin II precursor in frog and human reveals intense expression of the urotensin II gene

in motoneurons of the spinal cord. *Proc. Natl. Acad. Sci. U.S.A.* **1998**, *95*, 15803−15808.
(3) Ames, R. S.; Sarau, H. M.; Chambers, J. K.; Willette, R. N.; Aiyar, R. V.; Romanic, A. M.; Louden, C. S.; Foley, J. J.; Sauermelch, C. F.; Coatney, R. W.; Ao, Z.; Disa, J.; Holmes, S. D.; Stadel, J. M.; Martin, J. D.; Liu, W.-S.; Glover, G. I.; Wilson, S.; McNutty, D. E.; Ellis, C. E.; Eishourbagy, N. A.; Shabon, U.; Trill, J. J.; Hay, D. V. P.; Ohlstein, E. H.; Bergsma, D. J.; Douglas, S. A. Human urotensin-II is a potent vasoconstrictor and agonist for the orphan receptor GPR14. *Nature* **1999**, *401*, 282−286.
(4) (a) Marchese, A.; Heiber, M.; Nguyen, T.; Heng, H. H.; Saldivia, V. R.; Cheng, R.; Murphy, P. M.; Tsui, L. C.; Shi, X.; Gregor, P.; George, S. R.; O'Dowd, B. F.; Doehrty, J. M. Cloning and chromosomal mapping of three novel genes, GPR9, GPR10 and GPR14, encoding receptor related to interleukin 8, neuropeptide Y, and somatostatin receptors. *Genomics* **1995**, *29*, 335−344. (b) Tal, M.; Ammer, D. A.; Karpuj, M.; Krizhanovsky, V.; Naim, M.; Thompson, D. A. A novel putative neuropeptide receptor expressed in neural tissue, including sensory epithelia. *Biochem. Biophys. Res. Commun.* **1995**, *209*, 752−759.
(5) Libert, F.; Vassart, G.; Parmentier, M. Current developments in G-protein-coupled receptors. *Curr. Opin. Cell Biol.* **1991**, *8*, 218−223.
(6) (a) Nothacker, H. P.; Wang, Z.; McNeill, A. M.; Saito, Y.; Merten, S.; O'Dowd, B.; Duckles, S. P.; Civelli, O. Identification of the natural ligand of an orphan G-protein coupled receptor involved in the regulation of vasoconstriction. *Nat. Cell Biol.* **1999**, *1*, 383−385. (b) Mori, M.; Sugo, T.; Abe, M.; Shimomura, Y.; Kurihara, M.; Kitada, C.; Kikuchi, K.; Shintai, Y.; Kurokawa, T.; Onda, H.; Nishimura, O.; Fujino, M. Urotensin II is the endogenous ligand of a G-protein coupled orphan receptor, SENR (GPR14). *Biochem. Biophys. Res. Commun.* **1999**, *265*, 123−129. (c) Liu, Q.; Pong, S.-S.; Zeng, Z.; Zhang, Q.; Howard, A. D.; Williams, D. R.; Davidoff, M.; Wang, R.; Austin, C. P.; McDonald, T. P.; Bai, C.; George, S. R.; Evans, J. F.; Caskey, C. T. Identification of urotensin II as the endogenous ligand for the orphan G-protein coupled receptor GPR14. *Biochem. Biophys. Res. Commun.* **1999**, *266*, 174−178. (d) Davenport, A. P.; Maguire J. J. Urotensin II: fish neuropeptide catches orphan receptor. *Trends Pharmacol. Sci.* **2000**, *21*, 80−82.
(7) (a) MacLean, M. R.; Alexander, D.; Stirrat, A.; Gallagher, M.; Douglas, S. A.; Ohlstein, E. H.; Morecroft, I.; Polland, K. Contractile response to human urotensin-II in rat and human pulmonary arteries: effect of endothelial factors and chronic hypoxia in the rat. *Br. J. Pharmacol.* **2000**, *130*, 201−204. (b) Maguire, J. J.; Kuc, R. E.; Davenport, A. P. Orphan-receptor ligand human urotensin II: receptor localization in human tissues and comparison of vasoconstrictor responses with endothelin-1. *Br. J. Pharmacol.* **2000**, *131*, 441−446.
(8) Douglas, S. A.; Sulpizio, A. C.; Piercy, V.; Sarau, H. M.; Ames, R. S.; Aiyar, N. V.; Ohlstein, E. H.; Willette, R. N. Differential vasoconstrictor activity of human urotensin-II in vascular tissue isolated from the rat, mouse, dog, pig, marmoset and cynomolgus monkey. *Br. J. Pharmacol.* **2001**, *131*, 1262−1274.
(9) Maguire, J. J.; Davenport, A. P. Is urotensin-II the new endothelin? *Br. J. Pharmacol.* **2002**, *137*, 579−588.
(10) Douglas, S. A.; Ohlstein, E. H. Human urotensin-II, the most potent mammalian vasoconstrictor identified to date, as a therapeutic target for the management of cardivascular diseases. *Trends Cardiovasc. Med.* **2000**, *10*, 229−237.
(11) Hay, D.; Luttmann, M. A.; Douglas, S. A. Human urotensin-II is a potent spasmogen of primate airway smooth muscle. *Br. J. Pharmacol.* **2000**, *131*, 10−12.
(12) Russel, F. D.; Molenaar, P.; O'Brien, D. M. Cardiostimulant effects of urotensin-II in human heart in vitro. *Br. J. Pharmacol.* **2001**, *132*, 5−9.
(13) Douglas, S. A. Human urotensin-II as a novel cardiovascular target: "heart" of the matter or simply a fish "tail?" *Curr. Opin. Pharmacol.* **2003**, *3*, 159−167.
(14) (a) Grieco, P.; Rovero, P.; Novellino, E. Recent structure−activity studies of the peptide hormone urotensin-II, a potent vasoconstrictor. *Curr. Med. Chem.*, in press. (b) Carotenuto, A.; Grieco, P.; Rovero, P. Urotensin-II receptor peptide agonists. *Med. Res. Rev.*, in press.
(15) Grieco, P.; Carotenuto, A.; Campiglia, P.; Zampelli, E.; Patacchini, R.; Maggi, C. A.; Novellino, E.; Rovero, P. A new potent urotensin-II receptor peptide agonist containing a Pen residue at disulfide bridge *J. Med. Chem.* **2002**, *45*, 4391−4394.
(16) Grieco, P.; Campiglia, P.; Novellino, E.; Carotenuto, A.; Rovero, P.; Zampelli, E.; Patacchini, E.; Maggi, C. A. Urotensin-II (U-II) analogues containing modifications at disulfide bridge: Synthesis, biological and conformational studies. In *Peptides 2002*, Proceedings of the 27th European Peptide Symposium; Benedetti, E., Pedone, C., Eds.; European Peptide Society: Sorrento, Italy, 2003; pp 118−119.
(17) Bhaskaram, R.; Arunkumar, A. I.; Yu, C. NMR and dynamical simulated annealing studies on the solution conformation of urotensin II. *Biochim. Biophys. Acta* **1994**, *1199*, 115−122.
(18) Flohr, S.; Kurz, M.; Kostenis, E.; Brkovich, A.; Fournier, A.; Klabunde, T. Identification of nonpeptidic urotensin II receptor antagonists by virtual screening based on a pharmacophore model derived from structure−activity relationships and nuclear magnetic resonance studies on urotensin II. *J. Med. Chem.* **2002**, *45*, 1799−1805.
(19) Grieco, P.; Carotenuto, A.; Patacchini, R.; Maggi, C. A.; Novellino, E.; Rovero, P. Design, synthesis, conformational analysis, and biological studies of urotensin II lactam analogues. *Bioorg. Med. Chem.* **2002**, *10*, 3731−3739.
(20) Wüthrich, K. *NMR of Proteins and Nucleic Acids*; John Wiley & Sons: New York, 1986.
(21) (a) Piantini, U.; Sorensen, O. W.; Ernst, R. R. Multiple quantum filters for elucidating NMR coupling network. *J. Am. Chem. Soc.* **1982**, *104*, 6800−6801. (b) Marion, D.; Wüthrich, K. Application of phase sensitive two-dimensional correlated spectroscopy (COSY) for measurements of ^{1}H−^{1}H spin−spin coupling constants in proteins. *Biochem. Biophys. Res. Commun.* **1983**, *113*, 967−974.
(22) Bax, A.; Davis, D. G. Mlev-17-based two-dimensional homonuclear magnetization transfer spectroscopy. *J. Magn. Reson.* **1985**, *65*, 355−360.
(23) Jenner, J.; Meyer, B. H.; Bachman, P.; Ernst, R. R. Investigation of exchange processes by two-dimensional NMR spectroscopy. *J. Chem. Phys.* **1979**, *71*, 4546−4553.
(24) Bartels, C.; Xia, T.; Billeter, M.; Guentert, P.; Wüthrich, K. The Program XEASY for Computer-Supported NMR Spectral Analysis of Biological Macromolecules. *J. Biomol. NMR* **1995**, *6*, 1−10.
(25) Fairbrother, W. J.; Cavanagh, J.; Dyson, H. J.; Palmer, A. G., 3rd; Sutrina, S. L.; Reizer, J.; Saier, M. H., Jr.; Wright, P. E. Polypeptide backbone resonance assignments and secondary structure of *Bacillus subtilis* enzyme IIIglc determined by two-dimensional and three-dimensional heteronuclear NMR spectroscopy. *Biochemistry* **1991**, *30*, 6896−6907.
(26) (a) Wishart, D. S.; Sykes, B. D.; Richards, F. M. The Chemical Shift Index: A Fast Method for the Assignment of Protein Secondary Structure through NMR Spectroscopy. *Biochemistry* **1992**, *31*, 1647−1651. (b) Wishart D. S.; Bigam, C. G.; Holm, H.; Hodges, R. S.; Sykes, B. D. ^{1}H, ^{13}C, and ^{15}N random coil NMR chemical shifts of the common amino acids. Investigation of the nearest-neighbor effect. *J. Biomol. NMR.* **1995**, *5*, 67−81. (c) Andersen, N. H.; Liu, Z.; Prickett, K. S. Efforts toward deriving the CD spectrum of a 3(10) helix in aqueous medium. *FEBS Lett.* **1996**, *399*, 47−52.
(27) Guntert, P.; Mumenthaler, C.; Wüthrich, K. Torsion angle dynamics for NMR structure calculation with the new program DYANA. *J. Mol. Biol.* **1997**, *273*, 283−298.
(28) Hutchinson, E. G.; Thornton, J. M. PROMOTIF—A Program to identify and analyze structural motifs in proteins. *Protein Sci.* **1996**, *5*, 212−220.
(29) Weiβhoff, H.; Präsang, C.; Henklein, P.; Frömmel, C.; Zschunke, A.; Mügge, C. Mimicry of βII′-turns of proteins in cyclic peptapeptides with one and without D-amino acids. *Eur. J. Biochem.* **1999**, *259*, 776−788.
(30) Zampelli, E.; Carotenuto, A.; Grieco, P.; Campiglia, P.; Novellino, E. A.; Rovero, P. Urotensin-II: spectroscopic and molecular dynamics investigation in several environmental conditions. In *Peptides 2002*, Proceedings of the 27th European Peptide Symposium; Benedetti, E., Pedone, C., Eds.; European Peptide Society: Sorrento, Italy, 2003; pp 926−927.
(31) Croston, G. E.; Olsson, R.; Currier, E. A.; Burstein, E. S.; Weiner, D.; Nash, N.; Severance, D.; Allenmark, S. G.; Thunberg, L.; Ma, J. N.; Mohell, N.; O'Dowd, B.; Brann, M. R.; Hacksell, U. Discovery of the first nonpeptide agonist of the GPR14/urotensin-II receptor: 3-(4-chlorophenyl)-3-(2-(dimethylamino)ethyl)isochroman-1-one (AC-7954). *J. Med. Chem.* **2002**, *45*, 4950−4953.
(32) Maple, J.; Dinur, U.; Hagler, A. T. Derivation of Force Fields for Molecular Mechanics and Dynamics from Ab Initio Energy Surface. *Proc. Natl. Acad. Sci. U.S.A.* **1988**, *85*, 5350−5354.
(33) Rajan, R.; Awasthi, S. K.; Bhattachajya, S.; Balaram, P. Teflon-coated peptides: hexafluoroacetone trihydrate as a structure stabilizer for peptides. *Biopolymers* **1997**, *42*, 125−128.
(34) (a) Romano, R.; Dufresne, M.; Prost, M. C.; Bali, J. P.; Bayerl, T. M.; Moroder, L. Peptide hormone−membrane interactions. Intervesicular transfer of lipophilic gastrin derivative to artificial membranes and their bioactivities. *Biochim. Biophys. Acta* **1993**, *1145*, 235−242. (b) Moroder, L.; Romano, R.; Guba, W.; Mierke, D. F.; Kessler, H.; Delporte, C.; Winand, J.; Christophe, J. New evidence for a membrane bound pathway in hormone receptor binding. *Biochemistry* **1993**, *32*, 13551−13559.

(35) (a) Schwyzer, R. In *Natural Products and Biological Activities*; Imura, H., Goto, T., Murachi, T., Nakajima, T., Eds.; Tokyo Press and Elsevier: Tokyo, 1986; pp 197−207. (b) Schwyzer, R. Peptide−membrane interactions and a new principle in quantitative structure−activity relationships. *Biopolymers* **1991**, *31*, 785−792.

(36) (a) Sargent, D. F.; Schwyzer, R. Membrane lipid phase as catalyst for peptide−receptor interactions. *Proc. Natl. Acad. Sci. U.S.A.* **1986**, *83*, 5774−5778. (b) Schwyzer, R. Estimated conformation, orientation, and accumulation of dynorphin A-(1−13)-tridecapeptide on the surface of neutral lipid membranes. *Biochemistry* **1986**, *25*, 4281−4286. (c) Schwyzer, R. How do peptides interact with lipid membranes and how does this affect their biological activity? *Braz. J. Med. Biol. Res.* **1992**, *25*, 1077−1089.

(37) (a) Meraldi, J. P.; Hruby, V. J.; Brewster, A. I. R. Relative conformational rigidity in oxytocin and [1-penicillamine]-oxytocine: A proposal for relationship of conformational flexibility to peptide hormone agonism and antagonism. *Proc. Natl. Acad. Sci. U.S.A.* **1977**, *74*, 1373−1377. (b) Hruby, V. J. Conformational and topographical consideration in the design of biologically active peptides. *Biopolymers* **1993**, *33*, 1073−1082.

(38) Melacini, G.; Zhu, Q.; Goodman, M. Multiconformational NMR analysis of sandostatin (octreotide): Equilibrium between β-sheet and partially helical structures. *Biochemistry* **1997**, *36*, 1233−1241.

(39) Rossowski, W. J.; Cheng, B. L.; Taylor, J. E.; Datta, R.; Coy, D. H. Human urotensin II-induced aorta ring contractions are mediated by protein kinase C, tyrosine kinase and Rho-kinase: inhibition by somatostatin receptor antagonists. *Eur. J. Pharmacol.* **2002**, *438*, 159−170.

(40) Gill, S. C.; von Hippel, P. H. Calculation of protein extinction coefficients from amino acid sequence data. *Anal. Biochem.* **1989**, *182*, 319−26.

(41) Adler, A. J.; Greenfield, N. J.; Fasman, G. D. Circular dichroism and optical rotatory dispersion of proteins and polypeptides. *Methods Enzymol.* **1973**, *27*, 675−735.

(42) Koradi, R.; Billeter, M.; Wüthrich, K. MOLMOL: A Program for Display and Analysis of Macromolecular Structures. *J. Mol. Graphics* **1996**, *14*, 51−55.

JM0309912